Entanglement spectrum edge reconstruction and correlation hole of fractional quantum Hall liquids

Li-Xia Wei,[1] Na Jiang,[2] Qi Li,[3,4] and Zi-Xiang Hu[1,*]

[1]*Department of Physics and Center for Quantum Materials and Device, Chongqing University, Chongqing 401331, People's Republic of China*

[2]*Zhejiang Institute of Modern Physics, Zhejiang University, Hangzhou 310027, People's Republic of China*

[3]*Department of Physics, South University of Science and Technology of China, Shenzhen 518055, People's Republic of China*

[4]*School of Physics and Technology, Wuhan University, Wuhan 430072, People's Republic of China*

(Received 25 October 2019; revised manuscript received 24 December 2019; accepted 11 February 2020; published 27 February 2020)

The edge of the electronic fractional quantum Hall (FQH) system obeys the law of the chiral Luttinger liquid theory due to its intrinsic topological properties and the relation of bulk-edge correspondence. However, in a realistic experimental system, such as the usual Hall bar setup, the softening of the background confinement potential can induce the reconstruction of the edge spectrum, which breaks the chirality and universality of the FQH edge. The entanglement spectrum (ES) of the FQH ground state has the same counting structure as that of the energy spectrum indicating the topological characters of the quantum state. In this work, we report that the ES can also have an edge reconstruction while sweeping the area of the subsystem in real space cut. Moreover, we found that the critical area of the subsystem matches accurately with the intrinsic building block of the FQH liquids, namely the correlation hole of the FQH liquids. The above results seem to be universal after our study of a series of typical FQH states, such as two Laughlin states at $\nu = 1/3$ and $1/5$, and the Moore-Read state for $\nu = 5/2$.

DOI: 10.1103/PhysRevB.101.075137

I. INTRODUCTION

Topological states of matter have been a major theme in the recent developments in understanding novel quantum effects. The inherent fractional quantum Hall (FQH) effect [1,2] in high-mobility two-dimensional electron gases (2DEGs) under a strong magnetic field is a significant field to explore the topological phases. In these cases, the bulk of a FQH liquid is gapped, which results in the incompressibility of the topological quantum ground state [3,4]. However, low-lying gapless excitations exist at the boundary of the liquid, which provide a unique arena to study electron correlations in one dimension and topological properties in the bulk due to the bulk-edge correspondence in topological phases. It is known that topological states characteristically have protected edge states at the boundary between trivial and nontrivial regions. On the quantum Hall edge, the Fermi liquid theory breaks down and the edge electrons have been argued [5] to form the chiral Luttinger liquid (CLL). The CLL theory predicted that the current-voltage dependence in the tunneling between a Fermi liquid and a quantum Hall edge follows a universal power law $I \sim V^{\alpha}$, where $\alpha = m$ for the $\nu = \frac{1}{m}$ FQH states [6,7]. Such universality, however, has long been controversial since it has not been conclusively observed in semiconductor-based 2DEGs in spite of the fact that graphene-based 2DEGs have the potential to realize this universality [8,9]. One possible reason for this discrepancy is edge reconstruction [6,7], which induces additional nonchiral edge modes that are not tied to the bulk topology. Edge reconstruction is a consequence of the competition between the confinement potential that holds the electrons in the interior of the sample, and the Coulomb repulsion that tends to spread out the electron density. In numerical studies [10–14], the knob of the edge reconstruction was the distance between the 2DEGs and the background potential, or the strength of the confinement potential.

Another aspect to explore the edge excitation of the FQH state is the entanglement spectrum (ES) [15] of the ground-state wave function. The ES is the "energy spectrum" of the bipartite reduced density matrix of the ground state. It has a deep connection to the topological properties embedded in the ground state and its low-lying excitations. This connection is based on the conformal field theory (CFT) description of the FQH model wave functions, such as the Abelian Laughlin states at filling $\nu = 1/m$ and the non-Abelian Read-Rezayi states [16] with order-k clustering at filling $\nu = \frac{k}{kM+2}$. Mostly, the ES reveals the bulk topology via counting the low-energy excited states, which are regarded as the virtual edge excitation at the boundary of the bipartition. In analogy to the electron energy spectrum of an open boundary system, the counting numbers of the ES for the Laughlin state are "1, 1, 2, 3, 5, . . . " and "1, 1, 3, 5, 10, . . . " for the Moore-Read state, which can be predicted by CFT or CLL theory. However, except for the counting numbers, there are few studies on the quantitative properties of the ES, for example its edge velocities or edge reconstruction, and their relation to the bulk topology. This is because these properties are mostly believed to be nonuniversal and unrelated to the bulk topology.

The real-space bipartite cut [17–19] has the advantage of unambiguously determining the boundary between two

*zxhu@cqu.edu.cn

subsystems, which is helpful for quantification of the boundary length and subsystem area. Therefore, the real-space bipartition is the best way to fit the "area law" of the entanglement entropy and extrapolate the topological entanglement entropy [20–22]. In this paper, we systematically study the properties of the real-space ES of the FQH states in disk geometry. We find that the reconstruction of the ES can be realized by continuously tuning the position of the cut, namely the area of the subsystem with a fixed number of electrons in the subsystem. Interestingly, the critical area of the subsystem exactly matches the elementary unit of the fractional quantum Hall liquids. For example, the essential unit of the 1/3 Laughlin state is the electron bound to a correlation hole corresponding to "units of flux," or three of the available single-particle states that are exclusively occupied by the particle to which they are attached. In general, the elementary unit of the FQH liquid is a "composite boson" of p particles with q attached quanta, which is an analog of a unit cell in a solid. This conclusion is supported by our series of verifications, such as the model wave functions for the Laughlin state at $\nu = 1/3$ and 1/5 and the Moore-Read state [24] at $\nu = 5/2$ and their counterparts for Coulomb interaction.

The rest of the paper is organized as follows: In Sec. II, the model and the edge reconstruction are reviewed. The ES spectrum, its reconstruction, edge velocity, and subsystem entanglement entropy for the 1/3 Laughlin state are studied in Sec. III. The verifications for the realistic Coulomb interaction and other FQH states are considered in Sec. IV, and Sec. V gives the conclusions and discussions.

II. REVIEW OF THE MODEL AND EDGE RECONSTRUCTION IN THE ENERGY SPECTRUM

We consider a semirealistic microscopic model for FQH liquids in GaAl/GaAlAs heterostructure, which contains the 2DEGs layer located at the interface between GaAs and GaAlAs, and a uniform distributed positive background attributed to the dopants at a distance d in units of the magnetic length $l_B = \sqrt{\hbar c/eB}$. The background confinement competes with the electron-electron interaction, which is the driving force of the edge reconstruction. The density of the background charge is equal to the filling factor $\sigma = \nu$, and its overall charge cancels the charge of the electrons due to the charge-neutrality condition. Therefore, the background potential is a single body potential in the FQH problem. Without taking into account Landau level (LL) mixing and the spin degree of freedom for simplicity (the ground state is supposed to be spin-polarized), the Hamiltonian can be written as

$$H = \frac{1}{2}\sum_{\{m_i\}} V_{1234} c^\dagger_{m_1} c^\dagger_{m_2} c_{m_4} c_{m_3} + \sum_m U_m c^\dagger_m c_m, \tag{1}$$

where $c^\dagger_m$ is the electron creation operator for the lowest Landau level (LLL) single-electron state $\phi_m = |m\rangle$ with angular momentum m. The matrix element of two-body interaction and the background potential are

$$V_{1234} = \langle m_1, m_2 | V(r_1 - r_2) | m_3, m_4 \rangle \tag{2}$$

and

$$U_m = e\sigma \int_{r_2<R} d^2 r_2 \langle m | \frac{1}{\sqrt{d^2 + |\vec{r}_1 - \vec{r}_2|^2}} | m \rangle. \tag{3}$$

The advantage of this model is that, by tuning the parameters d, the FQH phases and their reconstructed edge states emerge naturally as the global ground state of the microscopic Hamiltonian without any explicit assumptions [10–12], e.g., on the value of the ground-state angular momentum. Thus we can study the stability of the phases and their competitions. Another advantage of the model is that we can analyze the edge excitations of the semirealistic system and identify them in a one-to-one correspondence with CLL edge theory or CFT [5,23]. For example, the low-lying excitations of the $\nu = 1/3$ Laughlin state can be described by a branch of single-boson edge states in CFT. Being edge excitations, such states can be independently verified by calculating the tunneling spectral weights and comparing them with the predictions of the CLL [11]. In addition to confirming the bulk topological order, we can use the microscopic calculation to extract energetic quantities, such as edge velocities, which are crucial for quantitative comparisons with experiments. The distance d between the 2DEGs and the uniform background potential is the parameter that tunes the relative strength between electron-electron repulsion and the attraction from the positive background. When d is small, the confinement is strong and electrons tend to stay in the interior of the sample, however the confinement becomes weaker while increasing d and thus the electrons, especially the ones near the edge, can spread out. This is the main mechanism of the edge reconstruction.

After projecting onto the LLL, the effective interaction of a two-body interaction can be expanded by a set of Haldane's pseudopotentials $\{V_m\}$ [25]. It is known that the Laughlin state at $\nu = 1/3$,

$$\Psi^3_L(\{z_i\}) = \prod_{i<j} (z_i - z_j)^3 e^{-\frac{1}{4}\sum_i |z_i|^2}, \tag{4}$$

is the exact zero-energy eigenstate for the V_1 model Hamiltonian. Another way of obtaining the model wave function is to use the Jack polynomials. It is known [26–28] that the FQH wave functions can be calculated recursively by Jack polynomials with a negative parameter α and a root configuration. The root configuration satisfies (k, r) admissibility, which means there can be at most k particles in r consecutive orbitals. For example, the root for the 1/3 Laughlin state is "1001001 $\cdots$" which has at most one electron in each of three consecutive orbitals. For electrons with Coulomb interaction at 1/3 filling, the edge reconstruction happens at $d \sim 1.5 l_B$ [10,11], which is signaled by a sudden change of the total angular momentum for the ground state as shown in Fig. 1. Previous numerical studies [10–12] show that the spectrum can be perfectly fitted by CLL theory for U(1) bosonic charge mode excitation [11]. The dispersion relations of the edge modes before and after reconstruction for systems containing from 6 to 10 electrons are shown in Figs. 1(c) and 1(d). The data for different systems are on one curve [12,29] and the extra edge modes are introduced at $\delta k \neq 0$, which leads to the nonuniversality of the FQH edge in the tunneling measurements.

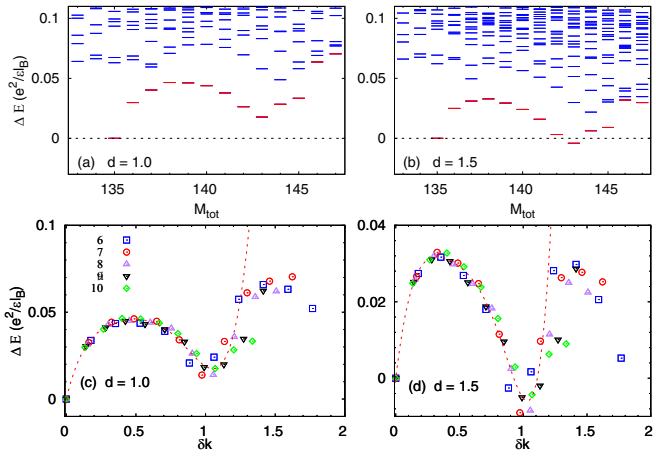

FIG. 1. The Coulomb energy spectrum for 10 electrons in 30 orbitals before (a) and after (b) edge reconstruction in disk geometry while tuning the background potential parametrized by d. The total angular momentum for the global ground state has an abrupt change from the Laughlin-like state with $M_{\rm tot} = M_0 = 3N(N-1)/2 = 135$ to $M_{\rm tot} = 143$ at the critical value of $d_c \sim 1.5 l_B$. Here we plot the spectrum with $\Delta E = E - E_0$ and $\Delta M = M_{\rm tot} - M_0$ in which E_0 is the ground-state energy in M_0 subspace. Parts (c) and (d) depict the dispersion relations of the edge mode in (a) and (b) for different system sizes.

III. EDGE RECONSTRUCTION IN THE REAL-SPACE ES

In this section, we move to the truncated space of the many-body quantum ground state. To obtain a bipartite system, a finite disk is divided into two parts as depicted in Fig. 2. A natural way of splitting the system is the orbital cut since the Hilbert space of the Hamiltonian in Eq. (1) is written in the basis of the Landau orbitals. However, the orbital cut appears as a fuzzy cut and not a sharp cut in real space. Several works [17–19] have addressed the sharp real-space partition. In this case, the electron operator can be written as

$$c_m = \alpha_m A_m + \beta_m B_m, \tag{5}$$

where A_m and B_m are the operators in the A and B subsystem, respectively. α_m^2 (β_m^2) is the electron distribution probability of the Landau wave function $|m\rangle$ in part A (B). In particular,

$$\alpha_m^2 = \int_0^{R_A}\int_0^{2\pi} |\phi_m(r,\theta)|^2 r\, dr\, d\theta = 1 - \frac{\Gamma\left(1+m, \frac{R_A^2}{2}\right)}{\Gamma(1+m)}, \tag{6}$$

and $\alpha_m^2 + \beta_m^2 = 1$, where $\Gamma(n,x)$ is the incomplete gamma function. The von Neumann entanglement entropy is defined as $S_A = -{\rm Tr}[\rho_A \log \rho_A]$, where $\rho_A = {\rm Tr}_B \rho$ is the reduced density matrix of the subsystem after tracing out the degrees of freedom in part B. If ρ_A is finite-dimensional and has eigenvalues $\lambda_1, \ldots, \lambda_n$, then $S_A = -\sum_i \lambda_i \log \lambda_i$. An alternative way of deriving the entanglement entropy is to perform a Schmidt decomposition of the many-body wave function $|\Psi\rangle = \sum_i e^{-\frac{1}{2}\xi_i} |\psi_A^i\rangle \bigotimes |\psi_B^i\rangle$ giving $\exp(-\frac{1}{2}\xi_i) = \sqrt{\lambda_i}$ as the singular values. Thus the entanglement entropy can be expressed as $S_A = \sum_i \xi_i \exp(-\xi_i)$. It is known [15] that the full structure of the "entanglement spectrum" (ES), which is the logarithmic Schmidt spectrum of level ξ_i, contains much more information about the entanglement between two halves than that from S_A only. It plays a key role in analyzing the topological order of the FQH state. The structure of the dominant terms in the Schmidt expansion is analogous to the low-energy excitations of a many-body Hamiltonian. Especially, for a model wave function such as Eq. (4), the counting per momentum sector of the ES is identical to the energy spectrum of the edge excitations, being due to the bulk-edge correspondence. Beyond the counting, one could ask whether the entanglement energies of the ES mimic the dispersion of the edge excitation and also have reconstruction. And if the edge reconstruction happens, what does that tell us about the bulk of the FQH liquid?

We consider the Laughlin wave function for a finite number of electrons on a disk, which can be obtained either from diagonalizing a V_1 model Hamiltonian or from the Jack polynomials. Because the cut we chose conserves the rotational symmetry, in analogy to the energy spectrum in Fig. 1, the ES for a given number of electrons in subsystem N_A and the radius of the circular cut R_A are shown in Fig. 3. Here we consider a Laughlin state for 10 electrons, and the subsystem contains half of the particles. Then the radius of the subsystem R_A is a parameter that we tuned. After subtracting the ground-state quantum number for subsystem $\Delta M = M_A - \frac{3N_A(N_A-1)}{2}$ in the horizontal axis and its entanglement energy $\Delta\xi_i = \xi_i - \xi_0$ in the vertical axis, as expected, the counting number for each momentum subspace is identical to that in the energy spectrum. In a finite system, we can then define the edge velocity [12,23,30] through the excitation energy $\Delta\xi(\Delta M = 1)$ of the smallest momentum mode with edge momentum $k = \Delta M/R_A = 1/R_A$, i.e., $v_E = (R_A/\hbar)\Delta\xi$ $(\Delta M = 1)$, where $R_A = \sqrt{2N_A/\nu}$ is the radius of the subsystem. As indicated by the arrows in Fig. 3, the entanglement edge velocity v_E, which is proportional to the slope of the arrows, is likely nonmonotonic as the radius R_A increases.

If we plot v_E as a function of R_A for each subsystem with fixed N_A, as shown in Fig. 4(a) for the 10-electron Laughlin state, there is a minimum for each subsystem labeled by arrows. Interestingly, while v_E takes the value of the minimum, the ES seems to have an edge reconstruction. This is shown in Fig. 3(b) for a subsystem with $N_A = 5$ electrons.

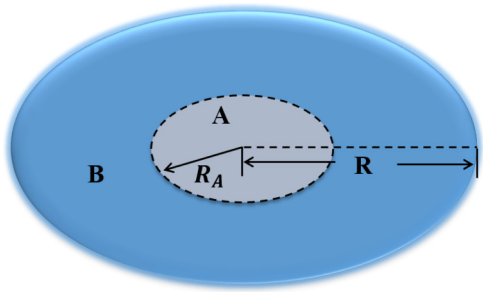

FIG. 2. The sketch map of a bipartite finite disk. The real space cut at the radius R_A conserves the rotational symmetry in perpendicular direction.

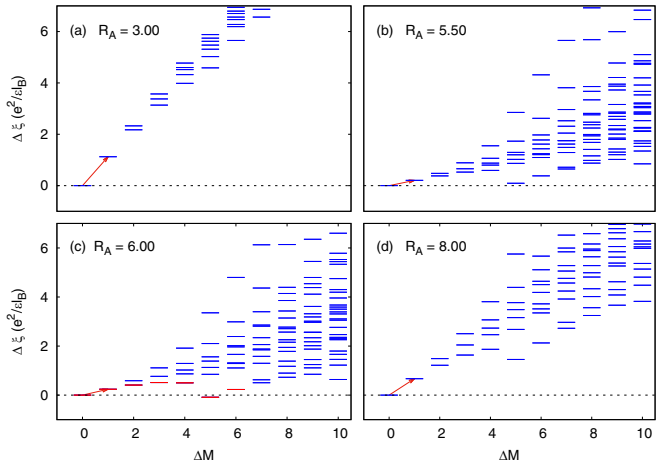

FIG. 3. The real-space ES for the 10-electron Laughlin state with $N_A = 5$ electrons in part A at different cuts. All the entanglement energies and angular momentum are subtracted by that of the ground state at $M = 30$. The edge reconstruction occurs near $R_A \sim 5.5l_B$, where the energy of the first excited state is almost the same as that of the ground state. The lowest edge states are plotted in red.

When $R_A \sim 5.5$, which is the minimum point as shown in Fig. 4(a), the lowest entanglement energy at $\Delta M = N_A = 5$ is roughly the same as that for the Laughlin state at $\Delta M = 0$. In Fig. 4(b), we pick out the minima values $v_{\min}$ in Fig. 4(a) and collect all the data from different systems ranging from 6 to 10 electrons. This shows us that the finite-size effect becomes small for large systems and especially in small subsystems. Therefore, in the thermodynamic limit, we believe that $v_{\min}$ saturates to a fixed value for each subsystem. According to the literature, another way of defining the edge velocity is by averaging the entanglement energy per angular momentum sector and extrapolating to the thermodynamic limit $N \to \infty$. It was shown that in this limit, the ES dispersion was compatible with a rescaling of the $\nu = 1$ edge mode velocity with a factor $1/\sqrt{3}$ [31].

In Fig. 5(a), we plot the average velocities in the thermodynamic limit for several subsystems N_A. Here the extrapolation is done with data from 6 to 10 electrons. This is reminiscent of Fig. 4(a), in which each subsystem still has a minimum that is more or less the same as that from the lowest two

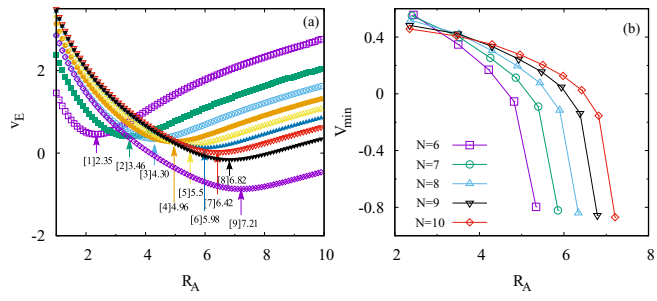

FIG. 4. (a) The edge velocities for a given subsystem as a function of R_A. The arrows and numbers label the minimum of the v_E for each subsystem. The number in the square brackets is N_A in the subsystem. (b) The minimum value of v_E vs R_A for systems ranging from 6 to 10 electrons.

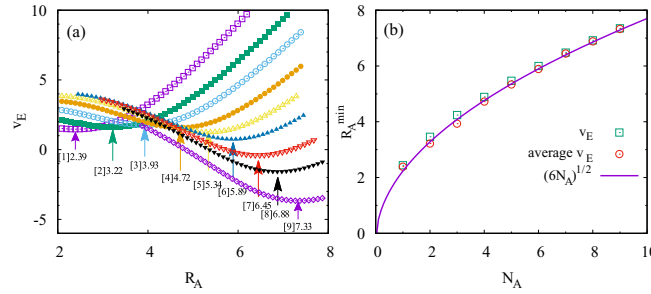

FIG. 5. (a) The average edge velocities for each subsystem as a function of R_A. The number in the square brackets labels the N_A. Each data point is determined by the extrapolation from the wave functions for 6–10 electrons. (b) Comparison of the edge velocities between using the lowest two states and the average value in each momentum sector. This shows that the results from both methods satisfy Eq. (7).

states in the ES. Similarly, the extrapolation can also be done from Fig. 4(b) for each subsystem. In Fig. 5(b), we plot these extrapolated critical edge velocities from the two methods. As expected, they are very close to each other and can be fitted very well by

$$R_A^{\min} = \sqrt{2N_A/\nu}. \tag{7}$$

This is because in the $\nu = 1/3$ Laughlin state, each electron sits in a correlation hole with an area containing three flux quanta. Thus for N_A electrons, there should be $3N_A$ flux quanta to form a correlation hole, which corresponds to a circular area with radius $\sqrt{6N_A}$.

According to the above analysis, in the real-space ES, in addition to the counting numbers per momentum subspace, the quantities of the edge spectrum still have significant physical meanings. For a fixed number of electrons, tuning the radius R_A, namely the area of the subsystem, can be the engine of the edge reconstruction in the ES. The critical area of the subsystem corresponds to the size of the correlation hole for N_A electrons. Now the nonmonotonic edge velocity v_E in Fig. 4 can be explained as follows: When $R_A = R_A^{\min}$, the electrons in both subsystems are balanced because the electron densities are equally distributed in the two regions. In this case, the low-energy excitation near the edge (the cut in the bipartition) should have the lowest energy cost. To gain more insight into the correlation hole, in the following we will try to obtain the critical radius of the subsystem from another aspect.

Subsystem entanglement entropy

Since the ES and the reconstruction we discussed above are restricted in a subsystem with a given N_A, we are naturally reminded that the subsystem entanglement entropy, which is the summation of all the energy levels in the ES for a given N_A, may have similar critical behaviors near $R_A^{\min}$. The subsystem entanglement entropy is defined as the entropy in a system with a given N_A,

$$S_{A,\mathrm{sub}}(N_A, R_A) = \sum_i \xi_{i,N_A} \exp(-\xi_{i,N_A}). \tag{8}$$

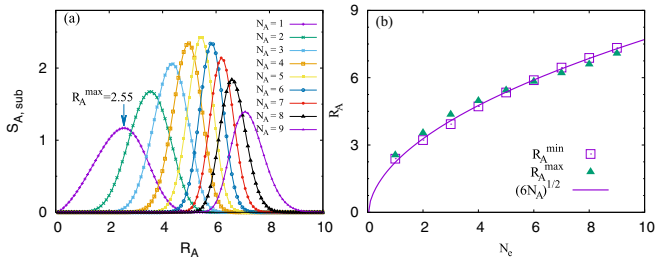

FIG. 6. (a) The subsystem entanglement entropy for a 10-electron Laughlin state. $R_A^{\max}$ labels the maximum values of $S_{A,\mathrm{sub}}$. (b) Comparison of $R_A^{\max}$ from the subsystem entanglement entropy and $R_A^{\min}$ from the minimizing edge velocity. Both are fitted very well by Eq. (7).

$S_{A,\mathrm{sub}}(N_A, R_A)$ as a function of R_A is depicted in Fig. 6(a). It shows that the subsystem entanglement entropy displays a Gaussian-like distribution as a function of R_A that has a maximum point $R_A^{\max}$ for each subsystem. Figure 6(b) presents a comparison of these maxima and the edge velocity minimum $R_A^{\min}$. It can be seen that the subsystem entanglement entropy only has a nonzero contribution near the edge of the correlation hole and is maximized exactly at the edge, or the correlation hole only has correlation (or entanglement) near its boundary. We remind the reader that the subsystem entanglement entropy is a partial entanglement entropy that cannot be used to apply the "area law" or extrapolate the topological entanglement entropy. The entanglement entropy should be the summation of $S_{A,\mathrm{sub}}(N_A, R_A)$ for all subsystems $N_A \in [0, N_e]$.

IV. COULOMB INTERACTION AND OTHER FQH STATES

A. Coulomb interaction

The analysis in the previous section is for the model wave function. Here we double-check the validity of the conclusions in the case of a realistic Coulomb interaction. We fix the background confinement at $d = 1.0l_B$ and calculate the real-space ES for each subsystem because the background potential has insignificant effects on the wave function of a gapped topological ground state. Recalling the model wave function, the entanglement velocity for the Coulomb interaction still has a minimum while increasing the radius of the circular cut R_A as depicted in Fig. 7(a). In Fig. 7(b), we

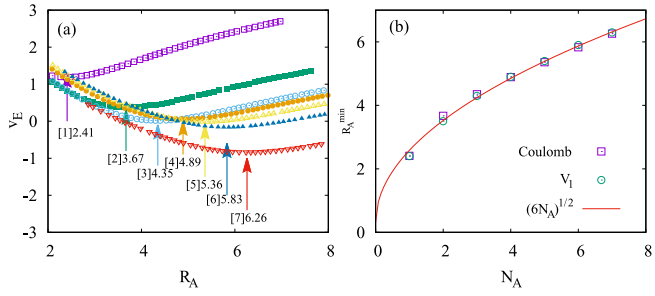

FIG. 7. The entanglement edge velocities as a function of R_A for Coulomb interaction (a) and its minimum values compared with that of the model wave function labeled by V_1 (b). Again, both are fitted very well by Eq. (7).

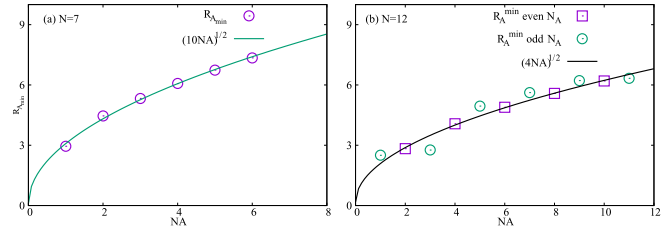

FIG. 8. By calculating the entanglement edge velocities and locating its minimum, the scaling of $R_A^{\min}$ for the 1/5 Laughlin state (a) and the Moore-Read state (b) still satisfies Eq. (7). The Moore-Read state has a strong even-odd effect in the edge velocity, which demonstrates the pairing properties of this non-Abelian state.

compare these extreme points with those from the model wave function via diagonalizing the V_1 Hamiltonian. It is shown that the Coulomb interaction is consistent with the model Hamiltonian and again obeys the relation $R_A^{\min} = \sqrt{2N_A/\nu}$.

B. Other FQH states

In the following, we consider the other two typical FQH states, namely the Laughlin state at $\nu = 1/5$ and the non-Abelian Moore-Read state, which is the candidate wave function for the $\nu = 5/2$ FQH state [24]

$$\Psi_L^5(\{z_i\}) = \prod_{i<j}(z_i - z_j)^5 e^{-\frac{1}{4}\sum_i |z_i|^2}, \tag{9}$$

$$\Psi_{\mathrm{MR}}(\{z_i\}) = \mathrm{Pf}\left(\frac{1}{z_i - z_j}\right)\prod_{i<j}(z_i - z_j)^2 e^{-\frac{1}{4}\sum_i |z_i|^2}. \tag{10}$$

The 1/5 Laughlin wave function is the model wave function for the two-body $\{V_1, V_3\}$ model Hamiltonian, and the Moore-Read Pfaffian wave function is the model wave function for the three-body V_3 model Hamiltonian. Of course, both of them can also be obtained from the Jack polynomials. In Fig. 8, we present the minimal edge velocity for different subsystems in two FQH states. Recalling the 1/3 Laughlin state, the results for the 1/5 Laughlin state scale very well with the relation $R_A^{\min} = \sqrt{10N_A}$, which demonstrates that the correlation hole of the 1/5 Laughlin state contains five flux quanta. The results for the Moore-Read state are shown in Fig. 8(b). Interestingly, from the macroscopic level, the equation $R_A^{\min} = \sqrt{4N_A}$ is satisfied, which means there are two flux quanta for each correlation hole in the Pfaffian state. Especially, the data for the even number of N_A exactly match this relation. However, the data for the subsystem with an odd number of electrons have obvious deviations. This definitely shows us the pairing mechanism of the Pfaffian state, i.e., the correlation hole of the Moore-Read state should be four flux quanta occupied by two electrons. This is the fundamental unit of the Pfaffian state, which is labeled by "1100" in the root of the Jack polynomial.

V. CONCLUSIONS AND DISCUSSIONS

In conclusion, we systematically studied the properties of the real-space entanglement spectrum, especially the entanglement velocity in the case in which we treat the ES as the edge excitation near the bipartite cut. On a finite disk, similarly to the edge reconstruction of the energy spectrum

while softening the background confinement, the ES for a given subsystem with a fixed number of electrons N_A can also have edge reconstruction while increasing the area of the subsystem. The ES edge reconstruction corresponds to the minimum of the edge velocity. In the case of a circular cut that conserves the rotational symmetry, the corresponding radius of the subsystem satisfies the relation $R_A^{\min} = \sqrt{2N_A/\nu}$, which demonstrates the size of the fundamental correlation hole in FQH states. Besides the $1/3$ Laughlin wave function, this conclusion is also supported by the realistic Coulomb interaction and other FQH model wave functions, such as the $1/5$ Laughlin state and the Moore-Read Pfaffian state. We thus conclude that the ES can tell us not only the counting number of the CFT edge states, but also much more about the physical properties of the FQH liquids, such as the edge reconstruction and the size of the fundamental correlation hole. Especially, the strong even-odd effects of $R_A^{\min}$ for the Moore-Read wave function are consistent with the pairing property of the state.

Here we should note that our study of the real-space ES is based on the circular cut in the bulk. This is because we are studying the isotropic FQH states that conserve the rotational symmetry in disk geometry. For the generalized isotropic FQH states that do not conserve the rotational symmetry [32], we believe the real-space cut should follow the geometric shape of the Landau orbitals. Moreover, for a general anisotropic FQH state that breaks both the rotational and translational symmetries [33], in spite of the fact that we cannot plot the ES in the momentum sector and explore the edge reconstruction without rotational symmetry, it is worthwhile to explore relation of the subsystem entanglement entropy and the intrinsic metric in the correlation hole in future work [34].

ACKNOWLEDGMENTS

This work is supported by National Natural Science Foundation of China Grants No. 11674041 and No. 11974064, and Chongqing Research Program of Basic Research and Frontier Technology Grant No. cstc2017jcyjAX0084. Q.L. acknowledges the support of the National Natural Science Foundation of China Grant No. 11474144. N.J. is supported by the National Natural Science Foundation of China Grant No. 11674282 and the Strategic Priority Research Program of Chinese Academy of Sciences Grant No. XDB28000000.

[1] D. C. Tsui, H. L. Störmer, and A. C. Gossard, Phys. Rev. Lett. **48**, 1559 (1982).
[2] R. B. Laughlin, Phys. Rev. Lett. **50**, 1395 (1983).
[3] S. M. Girvin and A. H. Macdonald, Phys. Rev. Lett. **54**, 581 (1985).
[4] J. K. Jain, *Composite Fermions* (Cambridge University Press, New York, 2007).
[5] X. G. Wen, Int. J. Mod. Phys. B **06**, 1711 (1992).
[6] C. de C. Chamon and X. G. Wen, Phys. Rev. B **49**, 8227 (1994).
[7] A. M. Chang, Rev. Mod. Phys. **75**, 1449 (2003).
[8] Z. X. Hu, R. N. Bhatt, X. Wan, and K. Yang, Phys. Rev. Lett. **107**, 236806 (2011).
[9] G. H. Li, A. L. Mayer, D. Abanin, L. Levitov, and E. Y. Andrei, Nat. Commun. **4**, 1744 (2013).
[10] X. Wan, K. Yang, and E. H. Rezayi, Phys. Rev. Lett. **88**, 056802 (2002).
[11] X. Wan, E. H. Rezayi, and K. Yang, Phys. Rev. B **68**, 125307 (2003).
[12] N. Jiang and Z. X. Hu, Phys. Rev. B **94**, 125116 (2016).
[13] S. Jolad and J. K. Jain, Phys. Rev. Lett. **102**, 116801 (2009).
[14] S. Jolad, D. Sen, and J. K. Jain, Phys. Rev. B **82**, 075315 (2010).
[15] H. Li and F. D. M. Haldane, Phys. Rev. Lett. **101**, 010504 (2008).
[16] N. Read and E. Rezayi, Phys. Rev. B **59**, 8084 (1999).
[17] A. Sterdyniak, A. Chandran, N. Regnault, B. A. Bernevig, and P. Bonderson, Phys. Rev. B **85**, 125308 (2012).
[18] J. Dubail, N. Read, and E. H. Rezayi, Phys. Rev. B **85**, 115321 (2012).
[19] I. D. Rodriguez, S. H. Simon, and J. K. Slingerland, Phys. Rev. Lett. **108**, 256806 (2012).
[20] A. Hamma, R. Ionicioiu, and P. Zanardi, Phys. Lett. A **337**, 22 (2005).
[21] A. Kitaev and J. Preskill, Phys. Rev. Lett. **96**, 110404 (2006).
[22] M. Levin and X.-G. Wen, Phys. Rev. Lett. **96**, 110405 (2006).
[23] X. Wan, Z. X. Hu, E. H. Rezayi, and K. Yang, Phys. Rev. B **77**, 165316 (2008).
[24] G. Moore and N. Read, Nucl. Phys. B **360**, 362 (1991).
[25] F. D. M. Haldane, Phys. Rev. Lett. **51**, 605 (1983).
[26] B. A. Bernevig and F. D. M. Haldane, Phys. Rev. Lett. **100**, 246802 (2008).
[27] B. A. Bernevig and F. D. M. Haldane, Phys. Rev. Lett. **101**, 246806 (2008).
[28] R. Thomale, A. Sterdyniak, N. Regnault, and B. A. Bernevig, Phys. Rev. Lett. **104**, 180502 (2010).
[29] Y. Zhang, Y.-H. Wu, J. A. Hutasoit, and J. K. Jain, Phys. Rev. B **90**, 165104 (2014).
[30] Z. X. Hu, E. H. Rezayi, X. Wan, and K. Yang, Phys. Rev. B **80**, 235330 (2009).
[31] N. Regnault, *Entanglement Spectroscopy and Its Application to the Fractional Quantum Hall Phases. Strongly Correlated Electrons* (Ecole Normale Supérieure de Paris–ENS, Paris, 2013).
[32] R. Z. Qiu, F. D. M. Haldane, X. Wan, K. Yang, and S. Yi, Phys. Rev. B **85**, 115308 (2012).
[33] F. D. M. Haldane, Phys. Rev. Lett. **107**, 116801 (2011).
[34] D. Ye and Z. X. Hu (unpublished).